Iraqi Journal of Science, 2025, Vol. 66, No. 8, pp: 3267-3283
DOI: 10.24996/ijs.2025.66.8.18

ISSN: 0067-2904

Integrating Reservoir Properties with Microfacies Analysis of the Mishrif Formation at Zubair Oilfield, Iraq

Fahad M. Al-Najm[1], Heba A. Al-Samer[1], Mayssa N. Shehab[2], Maher M. Mahdi[1*]
[1] *Department of Geology, College of Science, University of Basra, Basra, Iraq*
[2] *Department of Oil and Gas Engineering, College of Oil and Gas Engineering, Basrah University for Oil and Gas, Basrah, Iraq*

Received: 20/11/2023 Accepted: 28/8/2024 Published: 30/8/2025

Abstract

Six wells were selected in this study for the Mishrif Formation (Late Cenomanian - Early Turonian) in the Zubair oilfield in southern Iraq, which is considered one of the main reservoirs in the field, to study the microfacies and to evaluate the petrophysical properties. This study estimates shale volume, distribution (dispersed, laminar and structural), and formation effective porosity from well log data and cross-plots. The distribution of shale is mainly dispersed, and an increase in effective porosity values indicates the quality of the reservoir. The microfacies analysis and the Lucia plot demonstrate that the Mishrif Formation consists of four main Microfacies (Lime mudstone, Wackestone, Packstone and Grainstone) in wells Zb-40 and Zb-114 containing only the core. The logs interpretation shows that the Mishrif Formation consists mainly of clean limestone rocks. The composition was divided based on the qualitative and quantitative interpretation of the logs into three reservoir units (MA, MB1, MB2). MB2 was divided into MB2.1 and MB2.2 based on oil and water saturation ratio. The results of the petrophysical analysis showed that MB1 and MB2.1 were the best reservoir units in terms of oil saturation and porosity in the study wells.

Keywords: Zubair Oilfield, Mishrif Formation, Petrophysical Analysis, Reservoir Division, Microfacies, Iraq.

خصائص المكمن مع تحليل السحنات الدقيقة لتكوين المشرف في حقل الزبير النفطي، العراق

فهد منصور النجم[1]، هبة أحمد حنون[1]، ميساء نوري شهاب[2]، ماهر منديل مهدي[1*]
[1]قسم علم الارض, كلية العلوم, جامعة البصرة, البصرة, العراق
[2]قسم هندسة النفط والغاز , كلية هندسة النفط والغاز , جامعة البصرة للنفط والغاز , البصرة, العراق

الخلاصة

تم اختيار ستة آبار في هذه الدراسة لتكوين المشرف (السينوماياني المتأخر – التوروني المبكر) في حقل الزبير النفطي في جنوب العراق والذي يعتبر أحد الخزانات الرئيسة في الحقل، حيث درست السحنات الدقيقة

* Email: maher.mahdi@uobasrah.edu.iq

والعمليات التحويرية المؤثرة وقيمت الخصائص البتروفيزيائية.. اظهر المقطع التحليلي لمجس الكثافة والنيوترون ان توزيع صخر الزيتي في التكوين هو مشتت. تبين من خلال تحليل السحنات الدقيقة أن تكوين المشرف يتكون من أربع سحنات دقيقة رئيسية (سحنة الحجر الجيري الطيني، سحنة الحجر الجيري الواكي، سحنةالحجر الجيري المرصوص، سحنة الحجر الجيري الحبيبي) في الآبار Zb−40 وZb−114 الحاوية فقط على لباب. تم حساب الخواص البتروفيزيائية لتكوين مشرف باستخدام المجسات وتبين ان تكوين المشرف يتكون بشكل رئيسي من صخور الحجر الجيري النظيف، وتم تقسيمه إلى ثلاث وحدات مكامن (MA، MB1، MB2)، وتقسيم MB2 إلى MB2.1 وMB2.2a نسبة تشبع النفطي والمائي. واظهرت نتائج التحليل البتروفيزيائي ان الوحدة المكمنية MB1 و MB2.1 افضل وحدة مكمنية من حيث التشبع النفطي والمسامية في جميع ابار الدراسة

1. Introduction

The Zubair Oilfield in Southern Iraq is one of the most important. This field contains several reservoir units**,** especially in the Cretaceous period, represented by the Yammama, Zubair, and Mishrif formations [1]. The Mishrif Limestone Formation, along with the Zubair Formation, is considered one of the major reservoirs of an economy. It constitutes an oil reservoir due to its lithological features and geographical extensions in many fields, Southern and Central [2]. Zubair Oilfield is located in the southern part of Iraq, about 20 km west of the city of Basra, and is an extension of the field located between longitudes (47°28′30.8′′-47°49′40.8′′E) and two latitudes (30°03′46.8′′- 32°41′59.8′′N) [3]. The field is about 67 km long and 8.7 km wide, and its axis is parallel to the axis of the Rumaila Oilfield (in a Northwest-Southeast direction), extending from the Iraq-Kuwait borders to the marshes area North [4] (Figure 1).

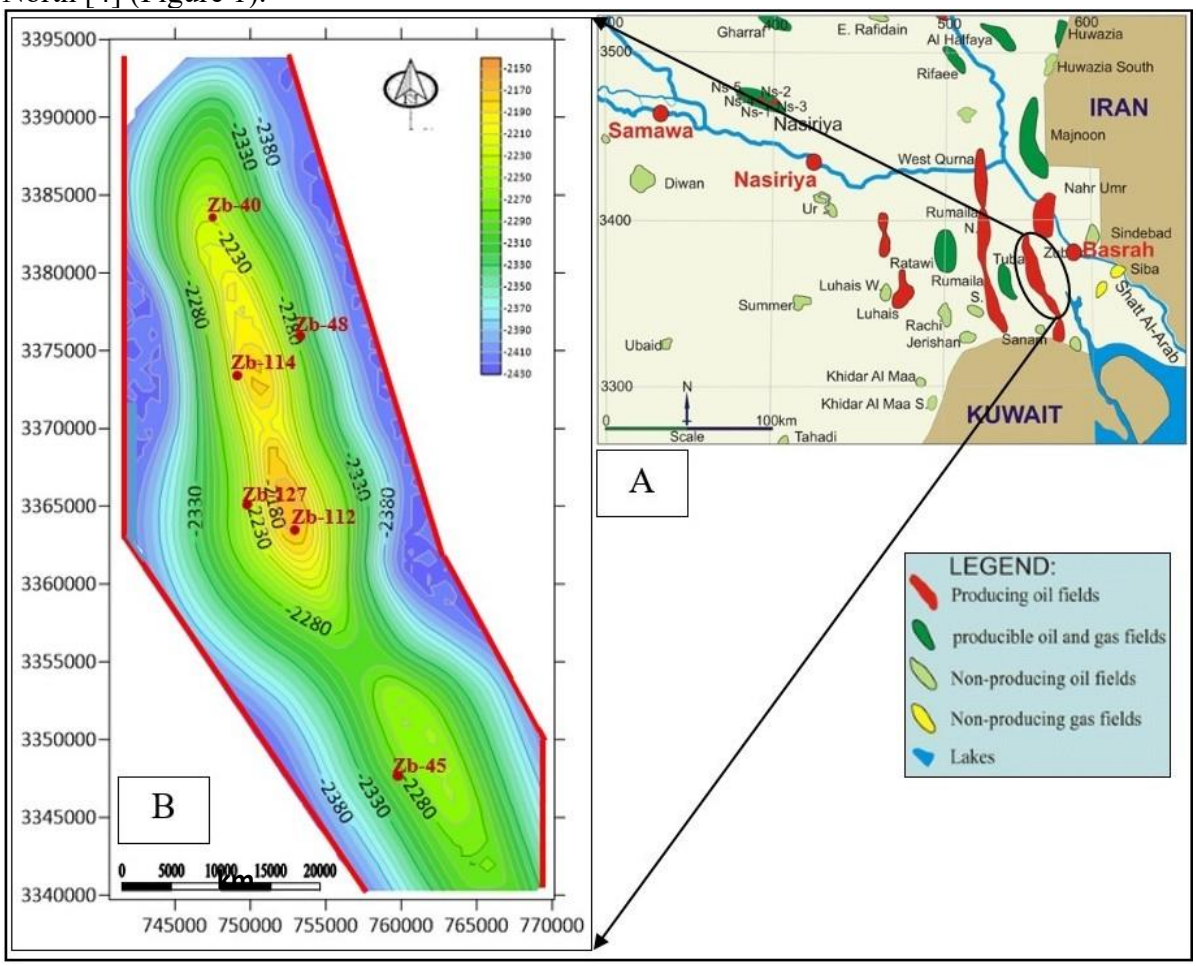

Figure 1: (A) Location map of the Zubair Oilfield, (B) Structural map for the Zubair Formation of the locations of the study wells.

Zubair oilfield is divided into four domes: Safwan, Al-Rafdhyia, Shuaiba, and Hammar [5 and 6]. Many studies focused on the Mishrif Formation because of its oil importance, and these are the most important studies [7]. The study aims to accurately determine the petrophysical characteristics and the microfacies for wells that do not contain cores by comparing them with two wells (Zb-40 and 114), with the electrofacies, thus dividing the reservoir into reservoir units depending on the inferred information.

2. Geological Setting

The Zubair Oilfield is located at the outer platform, in the Mesopotamian zone, exactly at the Zubair subzone [8 and 9]. It belongs to the Wasia group. The Mishrif Formation was deposited in the middle of the Cretaceous (Late Cenomanian – Early Turonian), which has the broadest conditions for producing hydrocarbons [10]. The formation comprises several lithology types, such as bioclastic, rudist, grey-white limestone, and a facies rich in Foraminifera that are capped with fossiliferous limestone [11]. It is bounded at the bottom in a manner compatible with the Rumaila Formation [12], while the upper surface represents a surface of disconformity with the Khasib Formation (Figure 2).

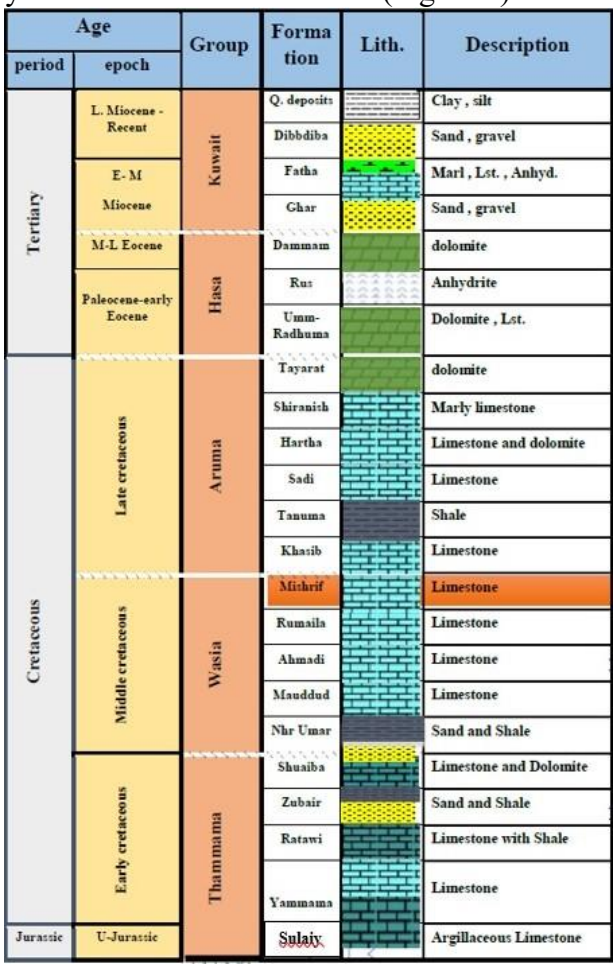

Figure 2: Stratigraphic column of Zubair Oilfield [13].

3. Materials and Methods

Six wells were selected in the Zubair Oilfield in southern Iraq (Zb-40, Zb-45, Zb-48, Zb-112, Zb-114 and Zb-127), as shown in Table 1 and Figure 1, taking into consideration in selecting the wells the availability of core data and the well logs (GR, CAL, Δt, RHOB, NPHI, Rt). The microfacies were determined for the wells in which core data were available (Zb-40 and Zb-114). More than 30 standard thin sections were made from these cores to determine the electrofacies. The Excel software was used to calculate the petrophysical

properties from the available well logs and then represent them in the Techlog software. Moreover, shale volume and porosity patterns were determined and distributed from well-log data based on a triangle density-neutron porosity cross-plot [14]. This cross-plot displays three distinct points (F, M, and SH); Point F is the fluid or water point where ØD = ØN =100% and M represents the matrix point; if ØN = ØD = 0. As point SH stands for the shale point, the coordinate of point SH [ØNSh, ØDSh] must be determined for the shale portion of the well. An important step in the facies analysis of calcareous reservoirs is describing and interpreting the cores. The available cores for the selected wells are described in Table 2. The description includes the nature of the lithology and facies, such as color, hardness, grain size, diagenetic processes, and oil evidence to determine the depositional environment.

Table 1: The boundaries, thicknesses and locations of wells of the Mishrif Formation in the Zubair Oilfield.

Well	Top (m)	Bottom (m)	Thickness (m)	Eastern (m)	Northern (m)	RTKB (m)	Core existence	Slides
Zb-40	2243.5	2392.0	148.5	747067	3384330	6.6	√	√
Zb-45	2299.2	2421.0	121.8	759826	3347987	18.3	×	×
Zb-48	2310.0	2465.8	155.8	753529	3376242	9.3	×	×
Zb-112	2196.5	2370.5	174.0	753010	3363147	26.7	×	×
Zb-114	2219.6	2380.0	160.4	749080	3373487	10.0	√	√
Zb-127	2240.8	2407.0	166.2	750482	3364788	20.8	×	×

Table 2: Depths of core intervals in the studied wells.

Zb-40		Zb-114	
Core NO.	**Intervals (m)**	**Core NO.**	**Intervals (m)**
C1	2245.1-2249.1	C1	2255.0-2259.1
C2	2282.6-2288.9	C2	2280.0-2286.2
C3	2270.0-2274.5	C3	2324.1-2328.7
C4	2345.0-2353.2	C4	2320.0-2323.5

4. Results

4.1. Qualitative Interpretation

The qualitative interpretation studies the behaviour of the curves of the open well logs used in the current study. The permeable and non-permeable layers and their thickness were determined through the SP log. As for the GR log, which measures the shale content in the formation, it was shown that the behaviour of the GR log in the wells of the study area indicates that the Mishrif Formation is considered one of the clean formations because the log readings are few except in some areas of the cap rocks that contain a percentage of shale figures 16 and 17. The lithology in the Mishrif Formation was determined using a density and neutron log. It consists primarily of limestone, with occasional dolomitic limestone layers at certain depths. Resistivity logs were employed to distinguish water-bearing zones from hydrocarbon-bearing zones, specifically indicating permeable zones [15]. The data points representing ØN and ØD values in clean formations (Vsh = 0) are located on the M-F line, and their position on the line indicates the effective porosity (PHIE) values. The points located on the M-SH line indicate the size of the shale volume for the formation with (PHIE = 0). The laminar, dispersed and structural shale points areas fall on or around LS-SH, DIS, and STR lines, respectively. Integration of neutron-density cross-plot analysis for reservoir units showed in Table 4 that shale distribution in the studied field is mainly dispersed shale,

and an increase in effective porosity values indicates the quality of the reservoir, as shown in Figures 3 and 4.

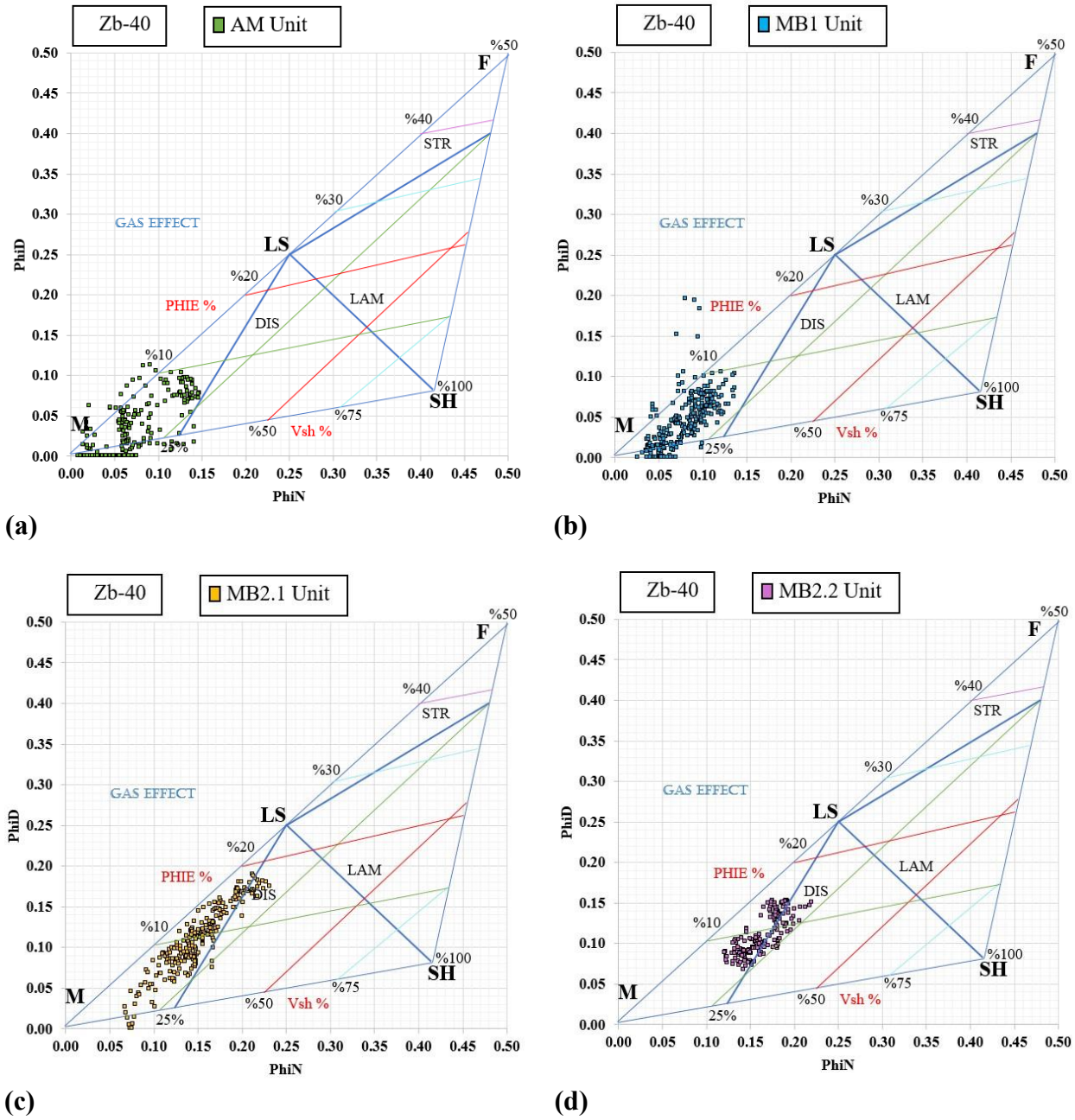

Figure 3: (a) Triangle density-neutron porosity cross-plot of MA unit, (b) MB1 unit, (c) MB2.1 unit,
(d) MB2.2unit in Zb-40.

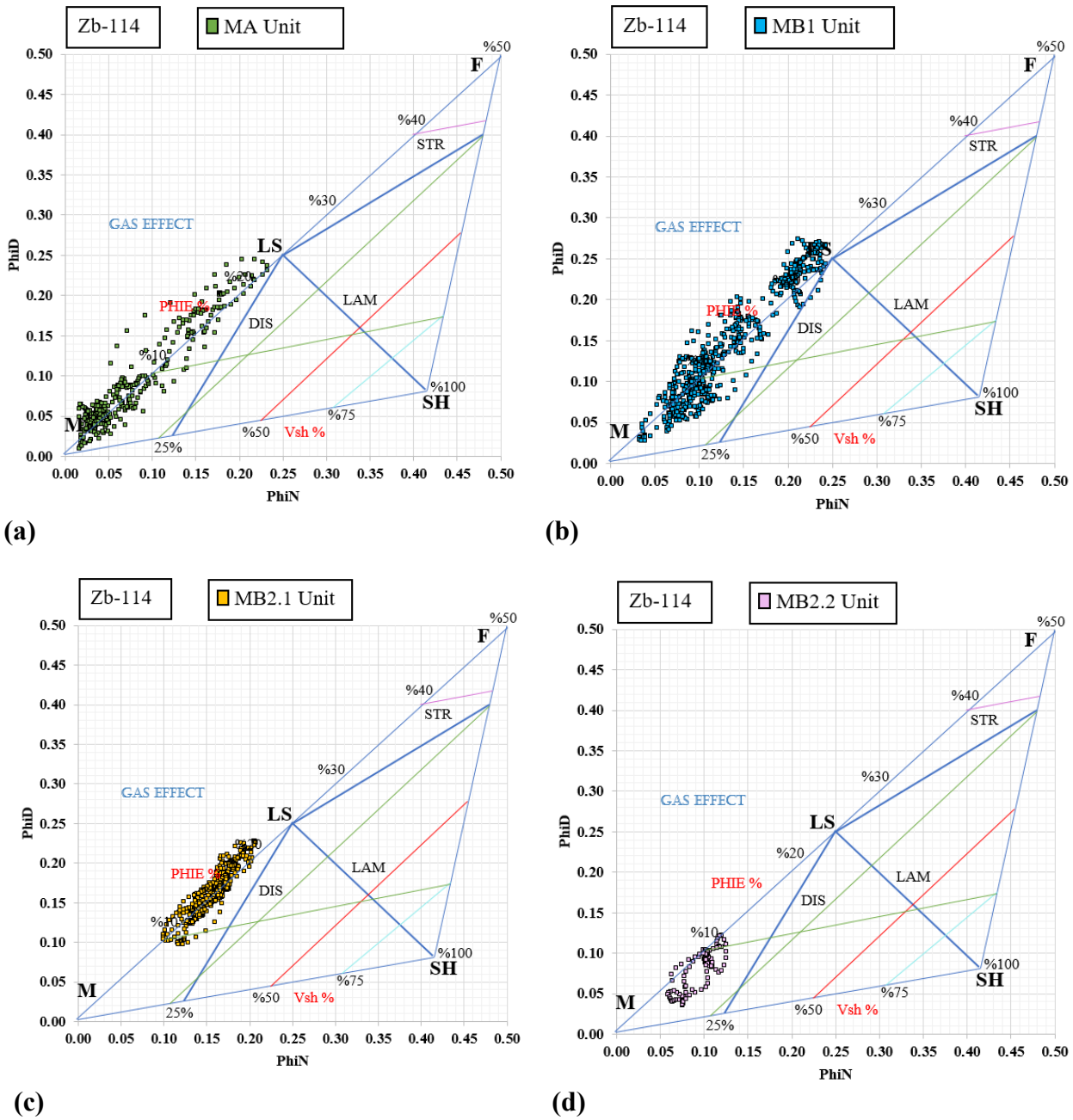

Figure 4: (a) Triangle density-neutron porosity cross-plot of MA unit, (b) MB1 unit, (c) MB2.1unit, (d) MB2.2unit in Zb-11.

4.1.1. Microfacies

Microfacies are the analysis of any stratigraphic sequence. The defined microfacies are a set of fossil and petrography resulting. The current study depends on [16] division to classify limestone in microfacies analysis because of its connection to the nature of the environmental energy depositing the facies.

The microfacies were determined for the wells in which cores were available Zb-40 and Zb-114 and then linked to electrofacies. The response and behaviour of the log are of great importance in interpreting the horizontal and vertical variation of the sedimentation process. Based on the behaviour and values of the log (Electrofacies), Microfacies were determined through the relationship between the gamma-ray log (GR) and density log (RHOB) and also

between the density log (RHOB) and neutron log (NPHI), as shown in Figure 5 and 6, as well as obtaining other properties such as clay content in rocks and porosity as shown in Table 3.

Table 3: Log response of Microfacies.

Energy		Microfacies	Elecrtofacies		
			Gamma-ray (GR) API unit	Density (RHOB) G/CC	Neutron (NPHI)% V/V
	Mud Support	Mudstone	50-70	2.6-2.7	0-6
		Wackestone	30-50	2.5-2.6	6-12
	Grain Support	Packstone	10-30	2.4-2.5	12-18
		Grainstone	<10	<2.4	>18

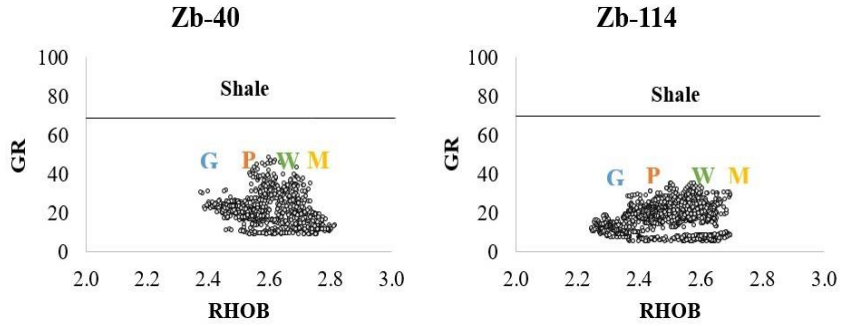

Figure 5- Determine microfacies of the gamma ray (GR) and density (RHOB) log.

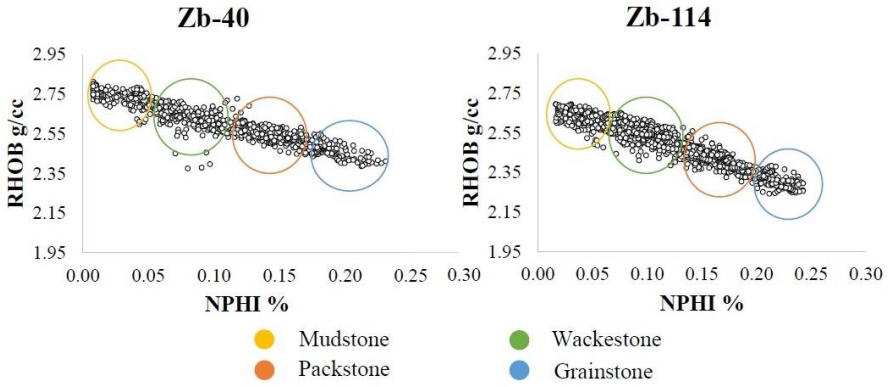

Figure 6: Determine microfacies of the gamma ray (GR) and density (RHOB) log.

(a) **(b)**

Figure 7: (a), (b) Microfacies succession of Mishrif Formation in Zb-40 well.

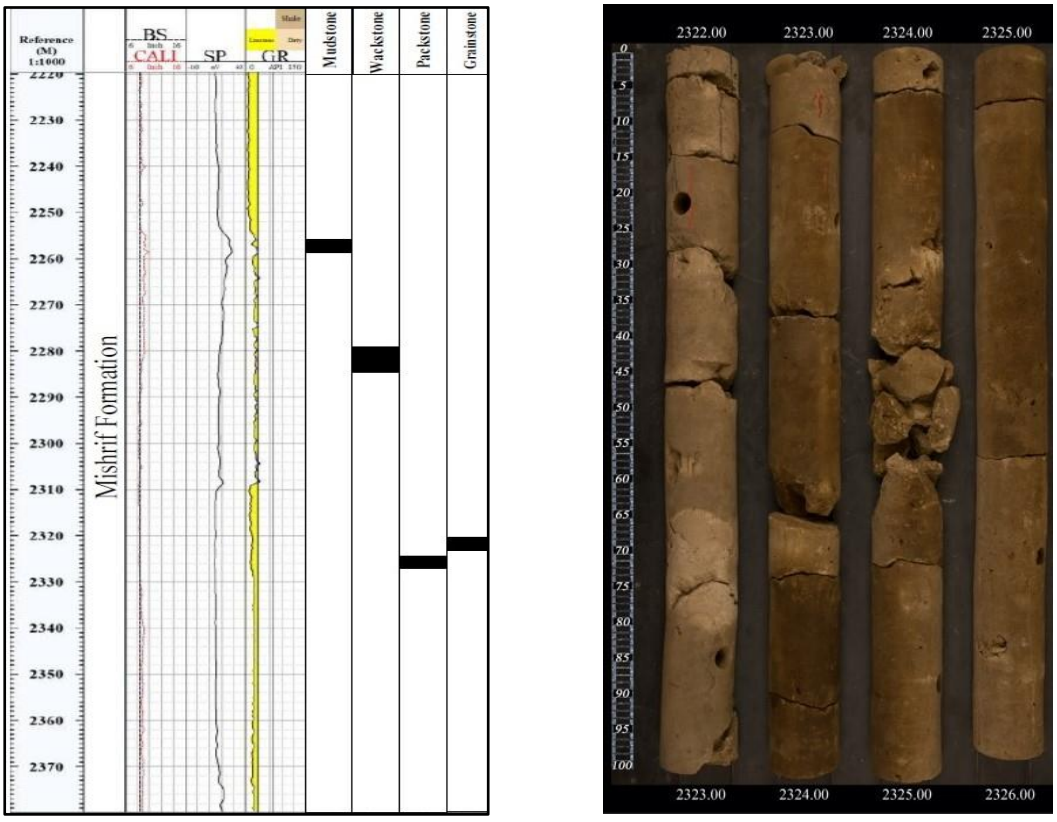

(a) **(b)**

Figure 8: (a), (b) Microfacies succession of Mishrif Formation in Zb-114 well.

Only the types of pores were linked to microfacies, but the environments of the different microfacies were not looked at in enough detail.

4.1.1.1. Lime Mudstone Microfacies

Lime Mudstones are laminated with black flint nodules. This facies contains fine-grained skeletal matter of less than 10%, and grains have been characterized by benthonic Foraminifera with fragments of large foraminifers that belong to the Alveolinids group (Figure 9). The sedimentation energy in these facies is very low due to mud, which indicates a poor reservoir unit.

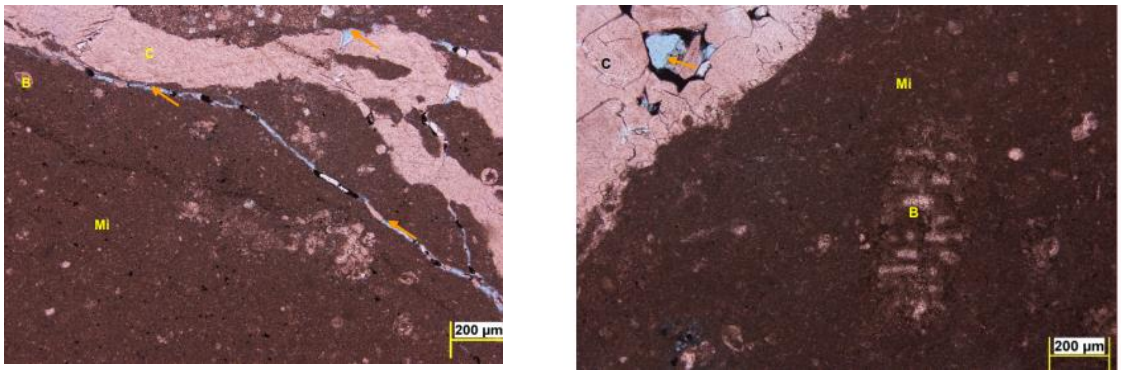

(a) **(b)**

Figure 9- (a) Lime mudstone microfacies in Zb-40, large channel porosity that filled in calcite spar, C: Calcite, Mi: micrite, B: benthic fossils, depth (2256m), b. Lime mudstone microfacies in Zb-40 and blocky cement fill the channel porosity with unfilled spaces and depth (2260 m).

4.1.1.2. Wackestone Microfacies

This facies is considered one of the most common facies of the section under study. This facies consists mainly of a micritic base with dispersion of dolomite. The dominant components are the benthic Foraminifera, echinoderms, molluscs and algae. It has also been noted that the porosity varies in this facies depending on the severity of its influence by diagenetic processes. The sedimentation energy in this facies is moderate, and its presence indicates a reservoir unit with moderate petrophysical characteristics. This facies was observed in the reservoir units (MA and MB1) in wells Zb-40 and Zb-114, as shown in Figure 10.

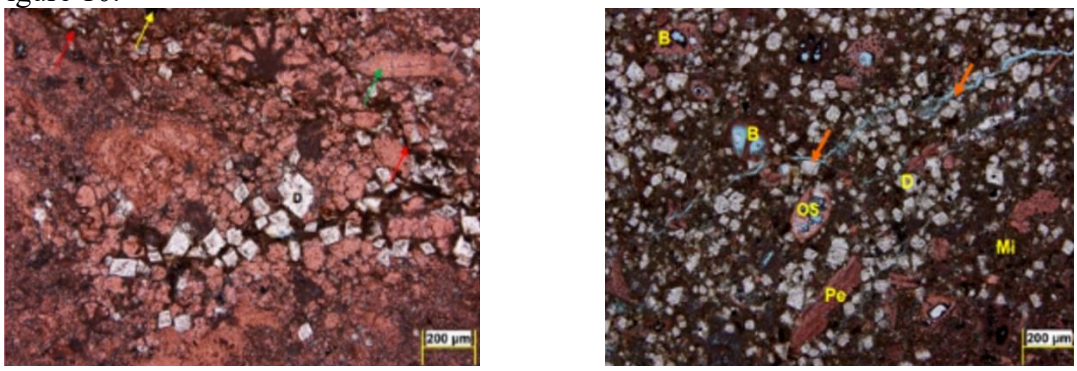

(a) **(b)**

Figure 10: (a) Wackestone microfacies in Zb-40, scattered rhomb of dolomite (D; dolomite), depth (2284.25m), (b) Wackestone microfacies in Zb-114, os: ostracods, pe: pelecypods, depth (2282.93m).

4.1.1.3. Packstone Microfacies

This type of facies is characterized by a high percentage of grains and pores, ranging between 70-90%). It is also characterized by grain support and depositing within a floor of the sprite. This facies generally reflect relatively high-energy depositional environments. This

facies indicates a good reservoir unit. It was observed to spread throughout the reservoir unit (MA) in Zb-40 and the reservoir unit (MB2.1) in Zb-114, as shown in Figure 11.

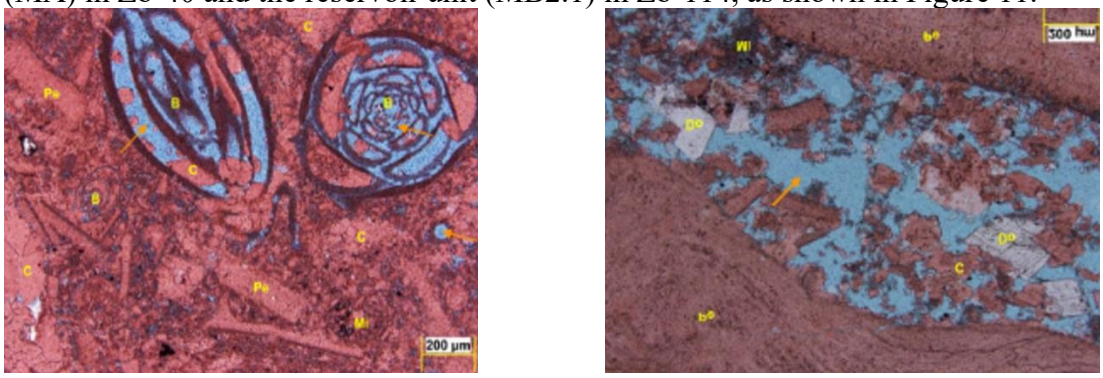

(a) **(b)**

Figure 11: (a) Packstone microfacies, Miliolids group with empty chambers that increase of porosity in Zb-40, depth (2272.30 m), (b) Packstone microfacies, empty channel porosity filled sometimes by blocky cements in Zb-114, depth (2326.15 m).

4.1.1.4. Grainstone Microfacies

This facies is characterized by an abundance of grains lying on top of each other in a fine calcite ground. The small and medium-sized skeletal grains range in high proportion between (90-100%) within a ground often composed of calcite. This facies generally reflect relatively very high-energy depositional environments. This facies indicates a very good reservoir unit. It was observed to spread throughout the reservoir unit (MB1) in Zb-40 and the reservoir unit (MB2.1) in Zb-114, as shown in Figure 12.

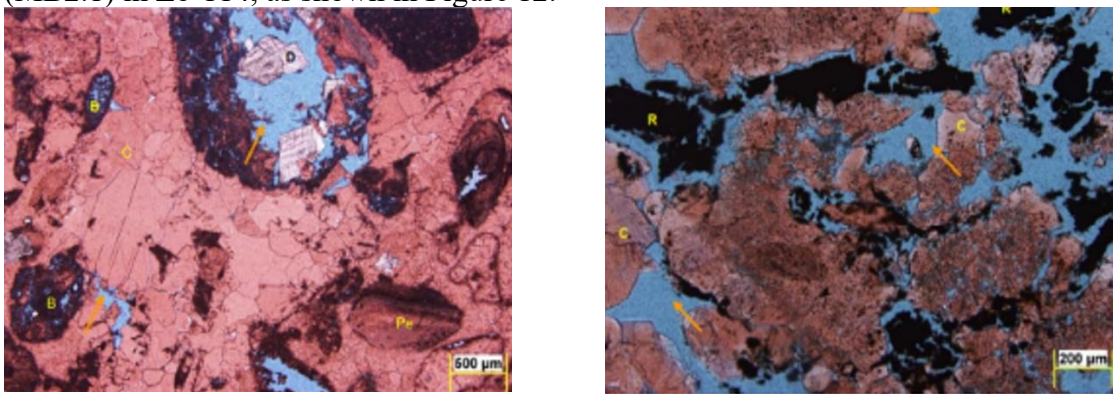

(a) **(b)**

Figure 12: (a) Grainstone microfacies in Zb-40, sparite groundmass and empty vugs created by dissolution fossils, depth (2293.83 m), (b) Grainstone microfacies, high porosity resulted of the dissolution in Zb-114, depth (2345.01 m).

4.2. Quantitative Interpretation

Using Excel software (2010) for the calculation of petrophysical properties of Mishrif Formation, then representation by using the Techlog software (2015), is obtained as below equations:

4.2.1 Calculation of Shale Volume (Vsh) [15].

$Vsh = (2^{(2*IGR)} - 1)/3$, **(1)**

Where Vsh = shale volume; IGR= gamma ray index.

IGR = (GR log – GR min)/(GR max – GR min), **(2)**

Where GR log = log reading (API); GR min = minimum GR; GR max = maximum gamma GR.

4.2.2 Calculating primary porosity from a Sonic log [17].

Øs = (Δt log - Δt ma)/(Δt f - Δt ma), **(3)**
Where Øs = Sonic–derived porosity; Δt log = formation measured by the log; Δt ma = the interval transit time in the rock matrix; Δt f = the interval transit time in the formation (induction=189).
Density porosity is calculated from a density log by using the Eq. (4) [18] and Eq. (5) [15].
ØD = (ρ ma – ρb)/(ρ ma – ρf) , **(4)**
ØDe = D ─Vsh × Dsh, **(5)**
Where ØD = density-derived porosity; ρ ma = matrix density (2.65); ρ b = the log reading; ρ f = fluid density (1); ØDe = Shale-corrected density porosity.
Neutron porosity is calculated directly from a neutron log using Eq. (6) [15].
ØNe = ØN ─ (ØNsh × Vsh), **(6)**
Where ØN = neutron porosity; ØNe = Shale-corrected porosity; ØNsh = neutron porosity of nearby shale.
4.2.3 The total porosity or effective porosity was calculated by Eq 7 in clean zones and Eq 8 in shale zones [19].
ØN.D = (ØN + ØD)/2, **(7)**
ØN.De = (ØNe + ØDe)/2, **(8)**
4.2.4 Secondary porosity was calculated [19].
SPI = ØN.D ─ ØS, **(9)**
4.2.5 Water and hydrocarbon saturation: Water saturation was calculated using Archie's equation 20. $SW = \sqrt{F * RW/Rt}$ **(10)**
$F = a / Ø^m$, **(11)**
Where SW = water saturation; Rt = true resistivity recorded by log (Ωm); Rw = formation water resistivity; F = formation factor; a = Tortuosity factor; m = Cementation factor.
The hydrocarbon saturation (Sh) is determined by the equation;
Sh = 1 ─ Sw, **(12)**
BVW = SW * ØN.D, **(13)**
BVh = Sh * ØN.D, **(14)**
Where, BVw = bulk volume water in the uninvaded zone; BVh = The total volume hydrocarbon.
(movable oil saturation), (residual oil saturation) [21]:
MOS = SXO ─ SW, **(15)**
ROS = 1 ─ SXO, **(16)**

5. Reservoir units of Mishrif Formation

The Mishrif Formation consists of successive units of limestone rocks of varying nature depending on their depositional environments, which were deposited during the (Late Cenomanian – Early Turonian). Based on the lithological examination of the core, published research, the reading of the logs and the results of the petrophysical calculations, the Mishrif Formation in the Zubair oilfield was divided into main reservoir units separated by non-reservoir units (insulating units) as follows: Cap rock 1 (CR1), Upper Mishrif (MA), Cap rock 2 (CR2), Middle Mishrif (MB1), Lower Mishrif (MB2).

- **MA Unit (Upper Mishrif):** This unit consists of fine-grained chalky limestone rocks in its upper parts. The thickness of this unit ranges between (15.0 m in Zb-127 to 52.0 m in Zb-48) with varying porosity for all study wells. The highest porosity and oil saturation rate value for this unit is in Zb-112, as shown in Table 4.

- **MB1 Unit (Middle Mishrif):** It consists of mainly chalky limestone rocks and granular limestone containing fossils. Its thickness ranges between (38.9 m in Zb-45 to 49.9 m in Zb-112). Different types of pores characterize it due to its impact on the secondary

dissolution process and subsequent diagenetic processes, leading to an increase in porosity in most parts of this unit. It is characterized by a high porosity with a value of (13.0 %) in the Zu-45 and Zb-114 with an average High oil saturation in the Zb-114 (Table 4).

- **MB2 Unit (Lower Mishrif):** This unit consists of granular limestone facies, compacted limestone, and compacted limestone, which contains some energetic foraminifera, algal remains, and fine grains. It is divided into two reservoir zones:

1) a reservoir zone of high hydrocarbon saturation MB2.1[22], the thickness ranges between (35.5 m in Zb-40 to 80.5 m in Zb-112).
This unit is characterized by high porosity, reaching the highest porosity value (19.0 %) in Zb-48 and average High oil saturation in the Zb-127 well.

2) Reservoir zone of high-water saturation MB2.2, the thickness ranges between (6.3 m in Zb-45 to 31.0 m in Zb-127), the highest porosity value (14.0 %) in Zb-40 and the rate of oil saturation is very few. It is non-existent as the rate of water saturation increases, which ranges between (90% - 100%) in the study wells (Table 4).

Table 4: Average petrophysical calculations for the reservoir units of the Mishrif Formation.

Well	Mishrif Unit	Top (m)	Bottom (m)	Thick (m)	Vsh	PHINDE	SH
Zb-40	MA	2243.2	2286.0	42.8	0.13	0.04	0.03
	MB1	2289.6	2330.6	41.0	0.35	0.05	0.01
	MB2.1	2330.6	2366.1	35.5	0.16	0.13	0.37
	MB2.2	2366.1	2392.0	25.9	0.16	0.14	0.00
Zb-45	MA	2299.2	2317.1	17.9	0.07	0.02	0.00
	MB1	2319.4	2358.3	38.9	0.02	0.13	0.11
	MB2.1	2358.3	2414.7	55.7	0.04	0.18	0.15
	MB2.2	2414.7	2421.0	6.3	0.04	0.05	0.00
Zb-48	MA	2310.0	2362.0	52.0	0.17	0.12	0.44
	MB1	2368.0	2407.7	39.7	0.39	0.11	0.21
	MB2.1	2407.7	2457.7	50.0	0.21	0.19	0.09
	MB2.2	2457.7	2465.8	8.1	0.21	0.13	0.01
Zb-112	MA	2196.5	2224.8	28.3	0.09	0.16	0.49
	MB1	2227.1	2274.0	46.9	0.42	0.11	0.45
	MB2.1	2274.0	2354.5	80.5	0.27	0.14	0.26
	MB2.2	2354.5	2370.5	16.0	0.23	0.11	0.06
Zb-114	MA	2219.6	2254.0	34.4	0.04	0.08	0.47
	MB1	2263.9	2308.9	45	0.40	0.13	0.55
	MB2.1	2308.9	2350.1	41.2	0.29	0.16	0.25
	MB2.2	2350.1	2380.0	29.9	0.27	0.09	0.01
Zb-127	MA	2240.8	2255.8	15.0	0.07	0.04	0.15
	MB1	2257.4	2307.3	49.9	0.09	0.12	0.47
	MB2.1	2307.3	2376.0	68,7	0.24	0.14	0.45
	MB2.2	2376.0	2407.0	31.0	0.17	0.13	0.10

6. Rocks Type

Lucia classified rock types according to pore size, sorting, porosity, and porosity of discrete interstices [23]. These properties give the pore size and distribution that controls permeability. The classification includes three categories of rock type: Class 1, characterized by a grain size of more than 100 micrometres and is roughly classified as grainstone; Class 2, the grain size ranges between 20–100 μm. This class is dominated by packstone, Class 3; the grain size is less than 20 μm. This class is dominated by pack-wackestone, wackestone, and lime mudstone (Figures 13 and 14).

Winland's equation, which is calculated from the logs and provides strong evidence for understanding the effectiveness of the reservoir units because it diagnoses the permeability of rocks, is a powerful method for utilizing reservoir properties such as permeability and porosity to classify the variety of rock types available in a reservoir [24 and 25].

Winland's R35 Equation is as follows:

$$\text{Log35} = 0.732 + 0.588 \log K_{air} - 0.864 \log Ø \quad \textbf{(17)}$$

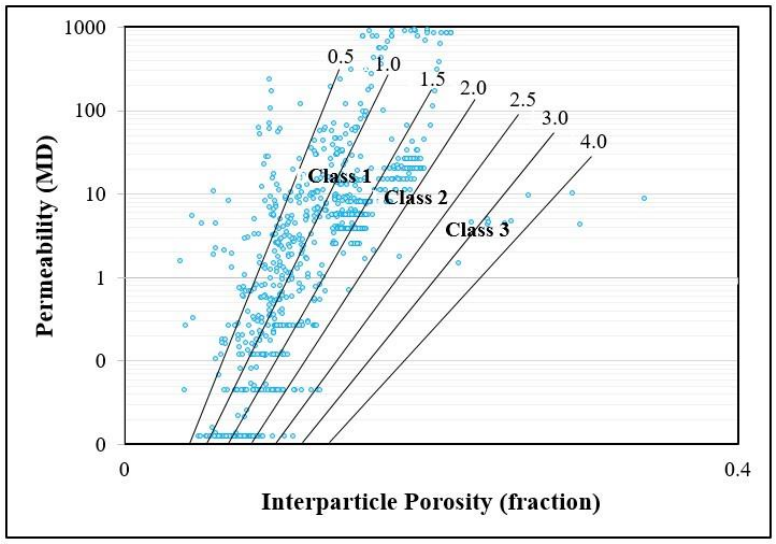

Figure 13: Rocks according to Lucia classification in Zb-40.

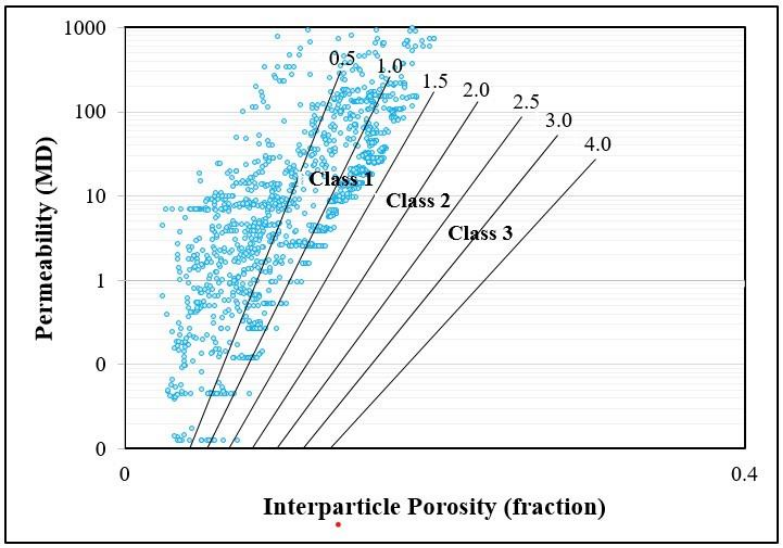

Figure 14: Rocks according to Lucia classification in Zb-114.

Where R35 = pore aperture when 35% mercury saturated; K air = air permeability; Ø= porosity.

pore throat radius can be divided into: (Figure 15)

1- Megapores: pore throat radius of more than 10 microns.
2- Macropores: pore throat radius between 2.5 and 10 microns.
3- Mesopores: pore throat radius between 0.5 and 2.5 microns.
4- Micropores: pore throat radius between 0.2 and 0.5 microns.
5- Nanopores: pore throat radius smaller than 0.2 microns.

The pore throat radius ranges from micropores to megapores. The megapores are referred to as grainstone when correlated with core data in a high-energy environment, while micropores are referred to as wackestone [26 and 27].

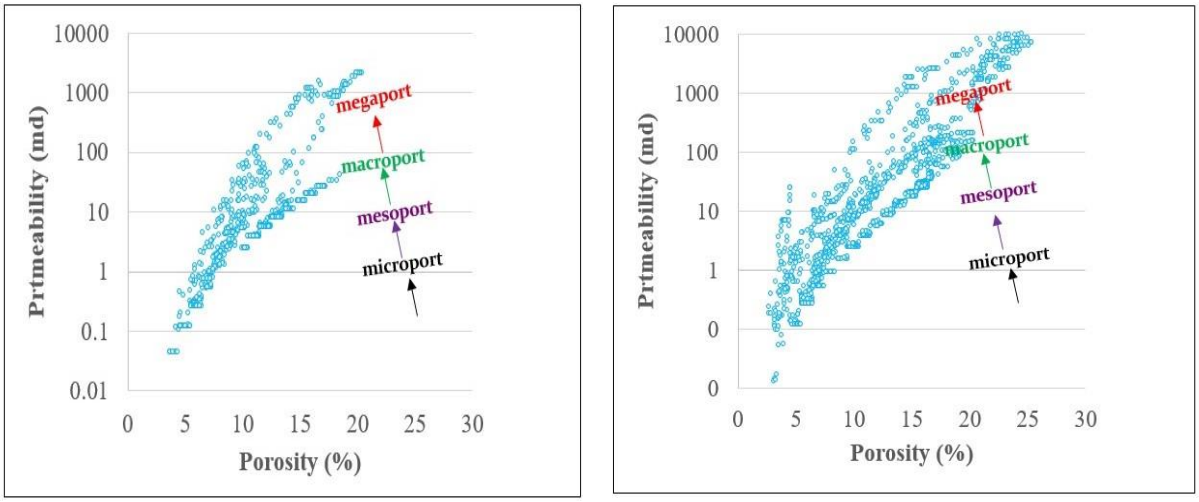

(a) **(b)**

Figure 15: (a) The relationship between Porosity and Permeability (R35) for Zb-40, (b) The relationship between Porosity and Permeability (R35) for Zb-114.

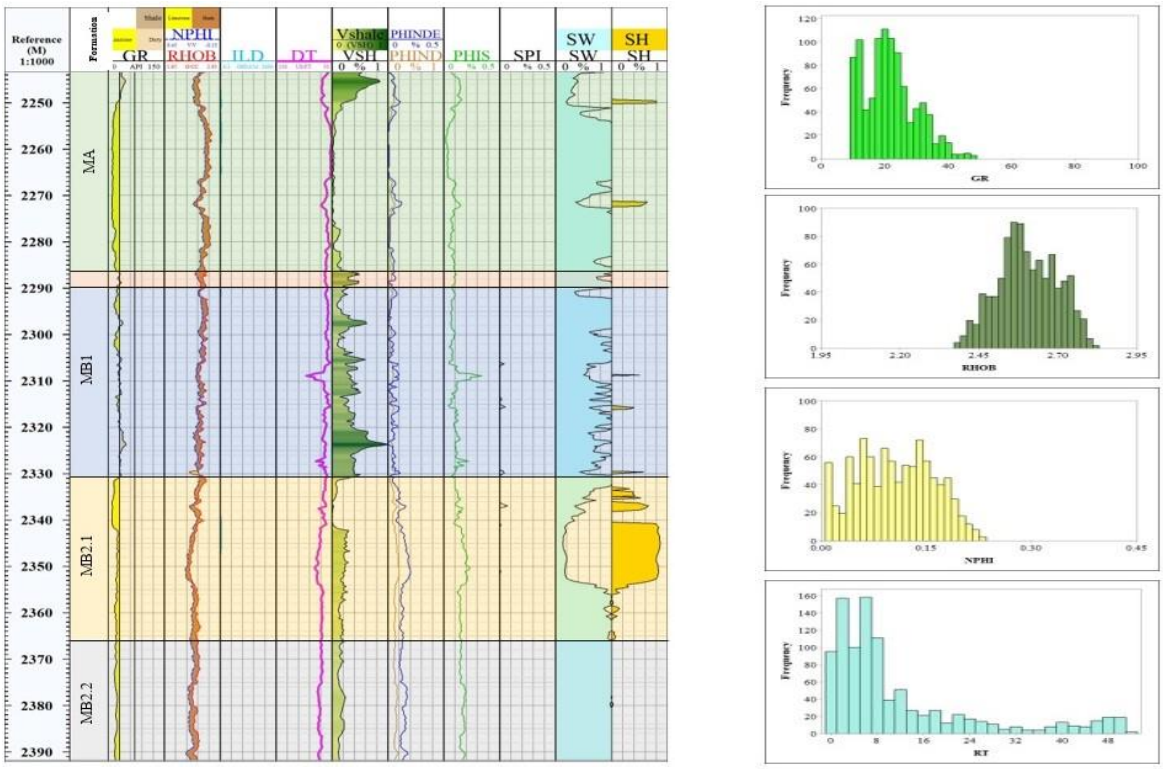

(a) **(b)**

Figure 16: (a) The behaviour of the well logs and the petrophysical result CPI for Zb-40, (b) Statistical interpretation of logs.

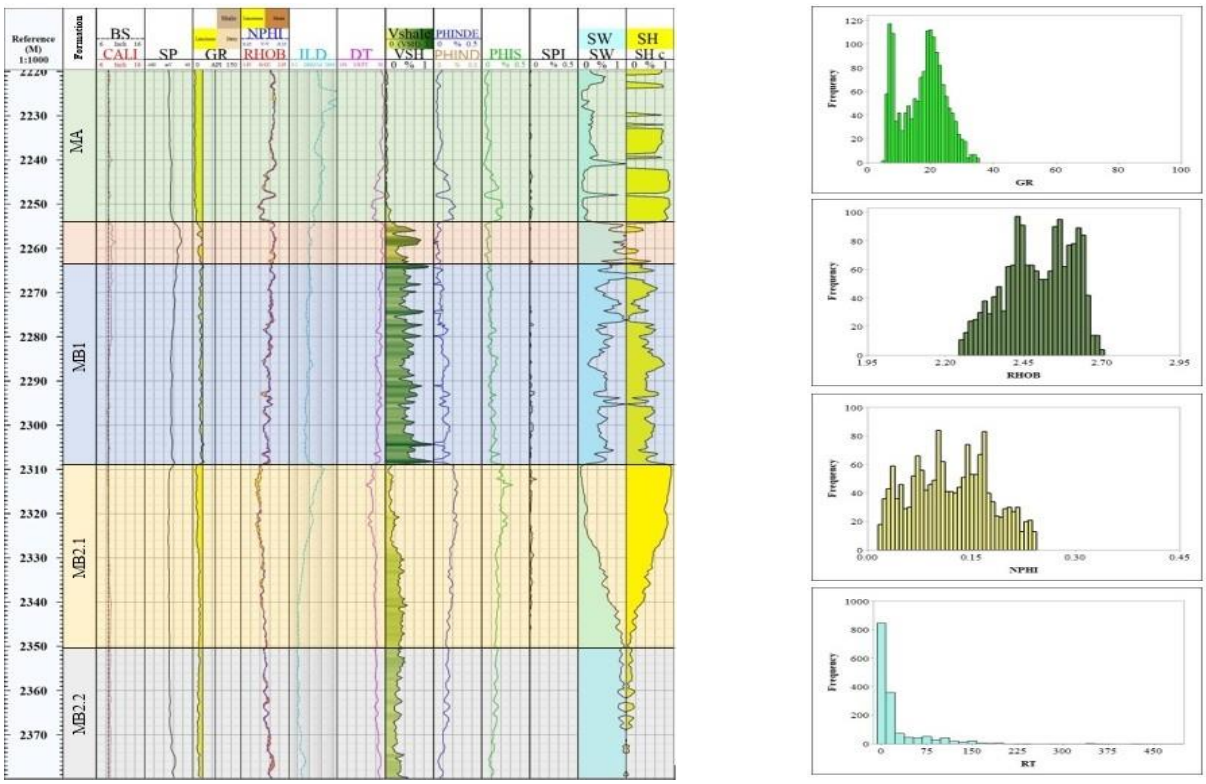

(a) **(b)**

Figure 17: (a) **T**he behaviour of the well logs and the petrophysical result CPI for Zb-114, (b) Statistical interpretation of logs.

7. Conclusions

The qualitative and quantitative interpretation showed that the Mishrif Formation in the Zubair field consists of clean limestone formations because the Gamma-ray log readings are few except in some areas of the cap rocks that contain a percentage of shale, and based on the behavior of the logs and the results of the petrophysical properties the Mishrif Formation was divided into three reservoir units (MA, MB1, MB2), MB2 was divided into MB2.1and MB2.2 based on oil and water saturation ratio, it is the MB1 and MB2.1best reservoir unit in terms of oil saturation and porosity in the study wells. Integration of neutron-density cross-plot analysis for reservoir units that shale distribution in the studied field is mainly dispersed shale, and an increase in effective porosity values indicates the quality of the reservoir. Based on electrofacies, core analysis and through the use of logs (Gamma-ray, Density, Neutron log) and comparing their specifications with microfacies and lithological descriptions from the core to determine the Microfacies and their distribution in wells Zb-40 and Zb-114 containing only the core, four main Microfacies of the rocks of the Mishrif Formation were identified, including (Lime mudstone, Wackestone, Packstone and Grainstone). By calculating the petrophysical characteristics of the reservoir, porosity and permeability, the types of rocks available in the reservoir were classified, and the pore throat radius was determined. The results showed that the reservoir rocks the pore throat radius range from micropores to megapores. Megapores are referred to as grainstone when correlated with core data in a high-energy environment, while micropores are referred to as wackestone.

References

[1] A. Al-Sayab, "Geology of petroleum ", Baghdad: University of Baghdad press, p.503, 1989.

[2] R. Idan, and A. L. Salih. "Reservoir Quality Related to Diagenetic Development in the Carbonate Mishrif Formation: A Case Study from the X Oilfield, Southern Iraq ". *Iraqi Geological Journal*, vol. 57, no.1A, pp.100-114, 2023.

[3] T. Mahdi, A. Aqrawi, A. Horbury, G. Al-Sherwani, "Sedimentological characterization of the mid-Cretaceous Mishrif reservoir in southern Mesopotamian Basin, Iraq ". GeoArabia vol.18, no.1, 2013.

[4] K. Ali, H. Husain, S. Shafik, "NORM in Markazia Degasing Station within North Rumaila Oilfield-Southern Iraq ". *Iraqi Journal of Science*, pp. 1464-1476., 2017.

[5] S. Jassim and J. Goff, "Geology of Iraq ", distributed by Geological Society of London, p.344, 2006.

[6] R. Owen, S. Nasr, "The stratigraphy of the Kuwait-Basrah area. In: Weeks, G.L. (Ed.), Habitat of Oil a Symposium ". AAPG, Tulsa, 1958.

[7] A. Aqrawi, G. Thehni, G. Sherwani, G.H., Kareem, B.A., "Mid-Cretaceous rudist-bearing carbonates of the Mishrif Formation: an important reservoir sequence in the Mesopotamian Basi ", Iraq. J. Petrol. Geol. Vol. 21, no. 1, 57e82, 1998.

[8] S. F. Fouad, S.F., "Tectonic map of Iraq, scale 1: 1000 000 ". *Iraqi Bulletin of Geology and Mining*, vol 11, no. 1, 2015.

[9] A. Handhal, M. Mahdi, "Basin modeling analysis and organic maturation for selected wells from different oil fields, Southern Iraq ". *Model. Earth Syst. Environ*. vol. 189 no. 2, 2016.

[10] M. Al-Kaabi, D. Hantoosh, B. Neamah, H. Almohy, Z. Bahlee, Mahdi, W. Abdulnaby, Classification of the Zubair Subzone oilfields using structural contour maps, Southern Iraq. *Journal of African Earth Sciences*, 197, 104770, 2023.

[11] S. Al-Dulaimi, A. Al-Zaidy, and S. Sa'ad, "The demise stage of rudist bearing Mishrif Formation (late Cenomanian–early Turonian), Southern Iraq". *Iraqi Bulletin of Geology and Mining*, vol. 9, no.3, pp.1-20, 2013.

[12] M. Al-Aaraji, H. Karim, " Structural Interpretation of Seismic Data of Mishrif Formation in East Abu-Amoud Field, South-eastern Iraq ". *Iraqi Journal of Science,* vol. 62, no. 10, pp. 3612-3619. 2021.

[13] H. K. Al-Mayyahi, "Sedimentological, mineralogical and geochemical study of upper shale member in Zubair formation - Rumaila oil field - south Iraq ", Science College, University of Basra.: Master thesis, 2018.

[14] W. H. Fertl, "Open hole cross plot concepts: A powerful technique in well log analysis ", *Journal of Petroleum* Technology, 1981.

[15] G. Asquith., and D. Krygowski, "Basic Well Log Analysis ", Published by The AAPG Tulsa, 2004.

[16] R. J. Dunham, "Classification of carbonate rocks according to depositional texture ": American Association of Petroleum Geologists Memoir, pp. 108-121.1962.

[17] M. Wyllie, A. R. Gregory, and G. H. F. Gardner. "An experimental investigation of the factors affecting elastic wave velocities in porous media," Geophysics, pp. 459-493. 1958

[18] A. Aqrawi, A. Horbury, Predicting the Mishrif reservoir quality in the Mesopotamian basin, southern Iraq. *GeoArabia*, vol. 13, no. 1, 2008.

[19] Schlumberger, " Log interpretation charts ", Houston: Schlumberger wire line, 1997.

[20] G. E. Archie, "The electrical resistivity log as an aid in determining some reservoir characteristics," *Petroleum Technology*, pp. 54-62, 1944.

[21] Schlumberger, "Log interpretation principles / Application, seventeen printing. Schlumberger Wireline & Testing 225, Texas 77478, 1998.

[22] M, Aziz, M Alwan, A. Al-Khafaji, and Q. Abeed, "The Mishrif reservoir characteristics utilizing well log data interpretation in the Fauqi Oilfield in Maysan, Southern Iraq.," *Iraqi Geological Journal*, vol. 55, no. 2E, pp. 82-95, 2022.

[23] F. J. Lucia, "Carbonate reservoir characterization. 2nd ed.," Spring, Berlin Heidelberg, 2007.

[24] K. J. Al-Qenae. "New approach for the classification of rock typing using a new technique for iso-pore throat lines in Winlands plot ", *Society of Petroleum Engineers*, 2015.

[25] R. Idan, and O. Al-Khazraji. "Characterization and Interpretation of Dedicated Reservoir Interval: A 2D Seismic Structural Approach", *Iraqi Journal of Science*, vol. 65, no. 3, pp. 1402–1411, 2024.

[26] M J. Ismail, F. Ettensohn, A. Handhal, A. Al-Abadi, "Facies analysis of the Middle Cretaceous Mishrif Formation in southern Iraq borehole image logs and core thin-sections as a tool ". *Mar. Petrol. Geol*. Vol. 133, no.2, 2021.

[27] R. Loucks, F. Lucia, L. Waite, "Origin and description of the micropore network within the Lower Cretaceous Stuart City Trend tight-gas limestone reservoir in Pawnee Field in south Texas ", 2013.